Atmos. Chem. Phys. Discuss., 11, 17759–17788, 2011
www.atmos-chem-phys-discuss.net/11/17759/2011/
doi:10.5194/acpd-11-17759-2011

Atmospheric
Chemistry
and Physics
Discussions

Predicting the relative humidities of liquid-liquid phase separation, efflorescence, and deliquescence of mixed particles of ammonium sulfate, organic material, and water using the organic-to-sulfate mass ratio of the particle and the oxygen-to-carbon elemental ratio of the organic component

A. K. Bertram[1], S. T. Martin[2], S. J. Hanna[1], M. L. Smith[2], A. Bodsworth[1], Q. Chen[2], M. Kuwata[2], A. Liu[1], Y. You[1], and S. R. Zorn[2]

[1]Department of Chemistry, University of British Columbia, Vancouver, BC CAN V6T 1Z1, Canada

[2] School of Engineering and Applied Sciences & Department of Earth and Planetary Sciences, Harvard University, Cambridge, Massachusetts, USA

Received: 5 June 2011 – Accepted: 8 June 2011 – Published: 23 June 2011

Correspondence to: A. K. Bertram (bertram@chem.ubc.ca)
S. T. Martin (smartin@seas.harvard.edu)

Published by Copernicus Publications on behalf of the European Geosciences Union.

Abstract

Individual particles that on a mass basis consist dominantly of the components ammonium sulfate, organic material, and water are a common class of submicron particles found in today's atmosphere. Here we use (1) the organic-to-sulfate (org:sulf) mass ratio of the overall particle and (2) the oxygen-to-carbon (O:C) elemental ratio of the organic component as input variables in parameterisations that predict the critical relative humidity of several different types of particle phase transitions. These transitions include liquid-liquid phase separation (SRH), efflorescence (ERH), and deliquescence (DRH). Experiments were conducted by optical microscopy for 11 different oxygenated organic-ammonium sulfate systems covering the range $0.1 <$ org:sulf <12.8 and $0.29 <$ O:C <1.33. These new data, in conjunction with other data already available in the literature, were used to develop the parameterisations SRH(org:sulf, O:C), ERH(org:sulf, O:C), and DRH(org:sulf, O:C). The parameterisations correctly predicted SRH within 15 % RH for 86 % of the measurements, ERH within 5 % for 86 % of the measurements, and DRH within 5 % for 95 % of the measurements. The applicability of the derived parameterisations beyond the training data set was tested against observations for organic-sulfate particles produced in an environmental chamber. The organic component consisted of secondary organic material produced by the oxidation of isoprene, α-pinene, and β-caryophyllene. The predictions of the parameterisations were also tested against data from the Southern Great Plains, Oklahoma, USA. The observed ERH and DRH values for both the chamber and field data agreed within 5 % RH with the value predicted by the parameterisations using the measured org:sulf and O:C ratios as the input variables.

1 Introduction

Atmospheric aerosol particles have many important roles in the Earth system. Examples include their feedback mechanisms to climate change, their links to the biogeochemical cycles of many elements, and their effects on regional visibility and human health (Finlayson-Pitts and Pitts, 1997; Ravishankara, 1997; Martin et al., 2004;

Pope and Dockery, 2006; Seinfeld and Pandis, 2006; Forster et al., 2007). In the atmosphere, single particles having both organic and sulfate species are abundant (Murphy et al., 1998; Buzorius et al., 2002; Murphy et al., 2006; Pratt and Prather, 2010). Since the sulfate fraction is often partially or fully neutralised by ammonium (Dibb et al., 1996; Huebert et al., 1998; Talbot et al., 1998; Dibb et al., 2000; Lee et al., 2003), mixed organic-ammonium sulfate particles constitute an important class of atmospheric aerosol particles.

Individual organic-ammonium sulfate particles can undergo liquid-liquid phase separation, efflorescence, and deliquescence as the relative humidity (RH) cycles between low and high values during air parcel motion and temperature oscillations in the atmosphere (e.g., Martin, 2000; Clegg et al., 2001; Brooks et al., 2002; Pankow, 2003; Parsons et al., 2004; Erdakos et al., 2006; Marcolli and Krieger, 2006; Ciobanu et al., 2009; Zuend et al., 2010; Smith et al., 2011). These phase transitions are illustrated in Fig. 1a. In the past, researchers trying to determine the phase transitions of organic-ammonium sulfate particles focused mainly on the individual organic molecules that have been identified in the atmosphere (e.g., Brooks et al., 2002; Wise et al., 2003; Braban and Abbatt, 2004; Parsons et al., 2006). In the atmosphere, however, the organic fraction in these mixed particles consists of 1000's of different molecules, with only about 10 % molecularly identified (Hallquist et al., 2009). Because only a small fraction of the organic material of atmospheric particles have been identified, liquid-liquid phase separation, efflorescence, and deliquescence of mixed organic-ammonium sulfate particles have been difficult to anticipate. Herein, given the intractability of characterising and studying 1000s of individual organic molecules, we explore a different approach by focusing on the organic-to-sulfate (org:sulf) mass ratio of the mixed particles and the oxygen-to-carbon (O:C) elemental ratio of the organic component as possible predictors of phase transitions. The practical advantage of using these ratios is that they are measured by instrumentation that has already been deployed at measurement sites worldwide (Jayne et al., 2000; Zhang et al., 2007; Aiken et al., 2008; Jimenez et al., 2009; Ng et al., 2010).

This presentation of the current study is structured, as follows. In Sect. 2, laboratory measurements of deliquescence, efflorescence, and liquid-liquid phase separation are described for particles containing one oxygenated organic molecule plus ammonium sulfate and water (i.e., three-component particles). Oxygenated organic molecules are a major fraction of the total organic particle mass concentration in the atmosphere, and they dominant relative to non-oxygenated organic molecules on a global-average mass basis (Kanakidou et al., 2005; Zhang et al., 2007; Hallquist et al., 2009). Each studied system consisted of one type of oxygenated organic molecule, plus ammonium sulfate and water (Tables S1–S3). Functional groups included esters, alcohols, carboxylic acids, ethers, and aromatics. This selection covers many of the functional groups found in the atmosphere (Finlayson-Pitts and Pitts, 1997; Seinfeld and Pandis, 2006; Day et al., 2009; Liu et al., 2009; Russell et al., 2011). In Sect. 3, the new laboratory results as well as other laboratory results reported in the literature are summarised and discussed, and the parameterisations of the laboratory results are presented. In Sect. 4, we apply the parameterisations to two case studies: an environmental chamber study and a field study. Section 5 presents conclusions and outlook.

2 Experimental

The relative humidity at which liquid-liquid phase separation (SRH), efflorescence (ERH), and deliquescence (DRH) occurred in 11 different oxygenated organic-ammonium sulfate systems was studied with an optical microscope coupled to a temperature controlled flow-cell (Pant et al., 2006; Ciobanu et al., 2009; Bodsworth et al., 2010). The bottom surface of the flow cell was a hydrophobic glass slide upon which the particles were deposited and observed. A solution of ammonium sulfate and an organic molecule was prepared in high-purity water or, in the case of low water-solubility organic molecules, in a mixture of water and methanol. The solution was then passed through a nebulizer to produce submicron droplets. These droplets were directed toward the hydrophobic glass slide, upon which they deposited and coagulated into supermicron droplets. The water or the water/methanol mixture was than evaporated to generate organic-ammonium sulfate particles with lateral dimensions ranging from 10 to 30 µm.

At the beginning of an experiment the RH in the flow cell was first set to nearly 100 %. Relative humidity was controlled by a continuous flow of a mixture of humid and dry N_2. Typical flow rates were approximately 1.5 L min^{-1}. After initialisation at nearly 100 % RH, the RH over the particles was then ramped down at a rate of 0.4–0.6 % per minute, and images of the particles were captured every approximately 20 s. The RH was decreased to approximately 25 % if efflorescence was observed and to as low as 2 % if no efflorescence was observed. After efflorescence was observed or the particles had been held at <2 % RH for some time, the RH was increased at the same rate to observe deliquescence of the particles. Calibration of the absolute RH readings was done using the DRH values for pure ammonium sulfate particles. All experiments were carried out at a temperature of 290 ± 1 K, except for experiments with 1,2,6-trihydroxyhexane. The results reported for 1,2,6-trihydroxyhexane were carried out at 273 ± 1 K, though several experiments were also conducted at 290 ± 1 K and confirmed that within experimental uncertainty the DRH, ERH, and SRH were the same at both temperatures.

The spatial distribution of the organic and sulfate material after liquid-liquid phase separation was probed with Raman microscopy. Raman spectra of a pure ammonium sulfate particle, a pure 4-dihydroxy-3-methoxybenzeneacetic acid particle, and a mixed 4-dihydroxy-3-methoxybenzeneacetic acid-ammonium sulfate particle (org:sulf of 3.1) were collected. Spectra were acquired on particles deposited on a hydrophobic glass slide in the same manner as for the optical microscope experiments. The spectra were collected using a Renishaw inVia Raman microscope with excitation using an argon ion laser at 514 nm and a power of 200 mW. All Raman spectra were collected at room temperature.

3 Laboratory results and discussion

Shown in Fig. 1b are examples of images recorded during a typical experiment in which liquid-liquid phase separation and efflorescence were observed (cf. Movie S1). The new data are plotted in Fig. 2 as a function of org:sulf and O:C, together with previous measurements of oxygenated organic-ammonium sulfate systems (Table 1 and references therein). Figure 2, as well as Figs. S1–S2, reveal that a dividing line emerges from the data, specifically for O:C < 0.7 compared to O:C > 0.7. For O:C < 0.7, the particles regularly undergo liquid-liquid phase separation, followed by efflorescence of the core with decreasing RH.

The spatial distribution of the organic and sulfate materials after liquid-liquid phase separation in a particle is shown in Fig. 3. The morphology is an organic coating surrounding an aqueous ammonium sulfate core, with small amounts of each in the other phase. This observation is consistent with the Raman spectra and optical images of poly(ethylene glycol)-ammonium sulfate particles after liquid-liquid phase separation (Ciobanu et al., 2009). In our studies, as well as the previous studies with poly(ethylene glycol)-ammonium sulfate particles, the hydrophobic glass slide may influence the morphology. Studies with levitated particles have observed other morphologies including an organic lens on a smaller aqueous droplet and several small aqueous ammonium sulfate inclusions suspended in an organic particle after liquid-liquid phase separation (Kwamena et al., 2010). Regardless of the morphology, the Raman spectra show that the nucleation-disrupting organic molecules are largely excluded from the aqueous salt after phase separation. This separation allows efflorescence to occur at an RH close to that of pure aqueous ammonium sulfate (Ciobanu et al., 2009; Smith et al., 2011).

The SRH value is independent of org:sulf in most cases, as illustrated in Fig. 2a and b, but correlates to first degree with O:C ($R^2 = 0.87$ for O:C ≤ 0.8; Fig. S2), at least for the parameter space explored here (i.e., $0.1 <$ org:sulf < 15 and $0.2 <$ O:C < 1.4). For O:C < 0.7, Fig. 2c demonstrates that as a first-order approximation ERH and DRH do not depend on org:sulf. Within experimental uncertainty, they are the same as those of pure ammonium sulfate. Conversely, for O:C > 0.7 Fig. 2d shows that ERH and DRH decrease with increasing values of org:sulf. ERH has greater sensitivity than DRH to increases in org:sulf.

The correlation between SRH and O:C shown in Fig. 2 and Fig. S2 can be rationalised by the salting out effect and the molar polarisation of the organic molecule. The decrease in solubility of an organic molecule in an aqueous solution due to the addition of a salt is known as the salting out effect. Salting out is described by Setchenov equation (Lee, 1997):

$$\ln \frac{S}{S_0} = k_\mathrm{s} C_\mathrm{s} \quad (1)$$

where S is the solubility of the organic molecule in the presence of the salt, S_0 is the solubility without the salt, C_s is the concentration of the salt, and k_s is the Setchenov constant. Increasingly negative values of k_s result in a greater tendency of an aqueous organic-inorganic particle to liquid-liquid phase separate. According to electrostatic theories, k_s is related to the molar polarization (P_m) of the organic molecule (Desnoyers and Ichhaporia, 1969). Since P_m is related to the polarisability and the dipole moment and, furthermore, since polarisability and dipole moment should be roughly related to O:C, one would expect a correlation between k_s and O:C and also a correlation between SRH and O:C. This line of thinking is also consistent with a recent modeling study using alcohols and salts that showed that hydrophilicity, which was reflected in O:C, is a key feature in defining the region of a miscibility gap (Zuend et al., 2010). The gap between 0.87 and unity for the correlation factor of SRH with O:C is plausibly explained by the combination of several different classes of organic molecules in our data set. A better correlation would be expected if a homologous series of organic molecules were studied.

In regard to the trends in DRH and ERH shown in Fig. 2, if a liquid-liquid phase separation occurs in a three-component system, the DRH and ERH values are expected to be closer to the binary system (inorganic and water) because in many cases after phase separation the organic molecules are expected to partition mostly to the organic phase. This expectation is supported by thermodynamic calculations and measurements (Clegg et al., 2001; Chang and Pankow, 2006; Ciobanu et al., 2009; Zuend et al., 2010). If liquid-liquid phase separation of a three-component system does not occur, a decrease in the DRH and ERH values of ammonium sulfate is expected with an increase in the org:sulf ratio, as implied by the Gibbs-Duhem relation. The Gibbs-Duhem relation states that an increase in the org:sulf ratio must correspond to an increase in the chemical potential of the organic material and a decrease in the chemical potential of ammonium sulphate for the assumption that activity coefficients do not behave atypically (Denbigh, 1981). The implication based on this relation for an increase in the org:sulf ratio are the following: a decreases in the solution saturation with respect to ammonium sulfate for a constant RH; a decrease in the DRH to maintain unity saturation; and a decrease in the ERH to maintain critical supersaturation.

The laboratory data listed in Table 1 and presented in Fig. 2 were parameterized as function of org:sulf and O:C. For O:C < 0.7, we fit the ERH and DRH values to a first-order polynomial in terms of both org:sulf and O:C. For O:C > 0.7, higher-order polynomials were required because ERH and DRH are stronger functions of these parameters over this range. At an org:sulf value of 0.1, ERH and DRH were fixed to 35 % and 80 % RH, respectively, to be consistent with the ERH of pure ammonium sulfate. For SRH, the data were parameterized using a second-order polynomial in O:C only. Figure 2a–b show that SRH is relatively insensitive to org:sulf. The parameterisations are included in Table 2 and are plotted in Fig. 4.

To evaluate the goodness-of-fit of the parameterisations, we calculated the reduced χ^2 values (see Table 2) as well as the residuals (Fig. 5). For ERH and DRH, the reduced χ^2 values were 2.62 and 1.09, respectively. Values close to 1 are considered good fits. The residuals appeared randomly distributed, as expected for good fits. For SRH, the reduced χ^2 values were larger (42.72), and the residuals were concentrated mainly between $0.5 <$ O:C < 0.7 and org:sulf > 1. The parameterisations correctly predict ERH and DRH within 5 % RH for 86 % and 95 % of the ERH and DRH measurements, respectively. We conclude that, to good approximation, trends in the ERH and

DRH of three-component organic-ammonium sulfate particles can be predicted with the presented parameterisations. The SRH parameterisation is less accurate: this parameterisation correctly predicts SRH within 15 % RH for 86 % of the measurements (Fig. 5). Nevertheless, the parameterisation does predict with reasonable accuracy the org:sulf and O:C parameter space where liquid-liquid phase separation is expected to occur. For more accurate predictions of SRH, a need for additional information (i.e., in addition to O:C) is indicated. Useful information would include organic functional groups and the organic molecular weight. However, any additional accuracy would come at the expense of added complexity in the parameterisation and may require chemical information that is currently not routinely measured (i.e., unlike org:sulf and O:C).

Measurements of average org:sulf and O:C by advanced on-line particle mass spectrometers have become available in the past few years for the central Amazon Basin (Chen et al., 2009) and for many locations in the Northern Hemisphere (Jimenez et al., 2009; Ng et al., 2010). Factor analysis has been used to separate the organic mass spectrum into hydrocarbon-like organic (HOA) and oxygenated organic (OOA) statistical components (Zhang et al., 2005, 2007; Jimenez et al., 2009). Since our parameterisations are applicable to the oxygenated component, we filtered the measurements (Chen et al., 2009; Jimenez et al., 2009; Ng et al., 2010) to include only those regions and times that had high OOA statistical scores compared to HOA scores. The constraint applied was OOA/(OOA+HOA) $\geq$0.85. The HOA component is believed to represented oily materials that have limited chemical interaction with oxygenated organic-sulfate-water components that are the focus of the present study. The sampling locations after filtering were: Riverside, Zurich (summer), Zurich (winter), off New England coast, Fukue, Okinawa, Cheju, Duke Forest, Pinnacle Park, Cheboque Point, Jungfraujoch, Hyytiala, and central Amazon Basin. For these locations, org:sulf and O:C campaign averages ranged from 0.36 to 5.39 and 0.43 to 0.85 respectively (Chen et al., 2009; Jimenez et al., 2009; Ng et al., 2010). Magenta boxes in Fig. 4 enclose the org:sulf and O:C range covered by these ambient measurements. Coincidence is apparent between (Chen et al., 2009; Jimenez et al., 2009; Ng et al., 2010) the locations of the magenta boxes representing ambient measurements and the org:sulf and O:C range covered by the introduced SRH, ERH, and DRH parameterisations.

4 Case studies

4.1 Environmental chamber studies

The applicability of the derived parameterisations for predicting the phase transitions of multi-component oxygenated organic-sulfate mixtures was tested using secondary organic material (SOM) that was mixed with sulfate and water in individual particles. The SOM was produced by the oxidation of volatile organic compounds (VOCs) in an environmental chamber in the presence of ammonium sulfate seed particles (Shilling et al., 2008; King et al., 2010; Li et al., 2011; Smith et al., 2011). Some of the oxidation products had low vapor pressures and consequently condensed onto the seed particles. Particle-phase SOM produced in an environmental chamber contains 10s to 100s of oxygenated compounds and as such represents a surrogate for atmospheric oxygenated organic material. Up to 90 % of the particle-phase submicron organic material in the atmosphere is SOM (Hallquist et al., 2009). The ERH and DRH of the mixed SOM organic-ammonium sulfate particles were measured using a tandem differential mobility analyzer (cf. Supplement and references Rosenoern et al., 2009; Smith et al., 2011). The org:sulf and O:C ratios were measured using on-line mass spectrometry (DeCarlo et al., 2006; Aiken et al., 2008; Shilling et al., 2009), including recent updates for SOM water peaks (Chen et al., 2011). Figure 6 shows both the ERH and DRH measurements (points) as well as the predictions (lines) obtained using the ERH and DRH parameterisations, with input parameters of the measured org:sulf and O:C. The derived parameterisations tested against the independent ERH and DRH measurements of the chamber particles were accurate within 3.4 % RH for all observations.

4.2 Field studies

The parameterisations were also tested against measurements that took place during June 2007 in the Southern Great Plains (SGP), Oklahoma, USA (cf. Supplement and references (Sheridan et al., 2001; Martin et al., 2008)). For the current analysis, we considered measurements for which the cation mole fraction arising from NH_4^+ was greater than 0.75 and the anion mole fraction arising from SO_4^{2-} was greater than 0.90. The use of this subset ensured that the inorganic composition was close to ammonium sulfate and that any deviations in the ERH and DRH from incomplete neutralisation or the presence of the nitrate anion were relatively small. Both of these factors have been demonstrated in laboratory studies to influence ERH and DRH (Martin et al., 2003). The org:sulf and O:C ratios at which efflorescence and deliquescence occurred at SGP are plotted in Fig. 4b and c, alongside the RH contours of the parameterisations. The parameterisations predict that ERH and DRH should lie within the ranges of 30–35 % and 75–80 %, respectively, in agreement with the observations at SGP.

5 Conclusions and outlook

The relative humidity at which liquid-liquid phase separation, efflorescence, and deliquescence occurred in 11 different oxygenated organic-ammonium sulfate systems was studied with an optical microscope. The new laboratory data as well as data reported in the literature was used to develop parameterisations in terms of O:C and org:sulf. The parameterisations correctly predict ERH and DRH for three component laboratory particles within 5 % RH for 86 % and 95 % of the measurements, respectively. The parameterisations correctly predict SRH within 15 % RH for 86 % of the measurements. Improvements in the predictions of SRH will require additional chemical information which may not be routinely measured. The applicability of the derived parameterisations for predicting the phase transitions of multi-component organic-ammonium sulfate mixtures were tested using environmental chamber data and field data from the Southern Great Plains, Oklahoma. The environmental chamber ERH and DRH data and field ERH and DRH data agreed with the parameterisations within 5 % RH.

The parameterisations presented herein represent a conceptual framework for the liquid-liquid phase separation, efflorescence, and deliquescence of a common class of atmospheric particles, specifically ammonium sulfate-organic-water particles. In outlook, this framework can be generalised to other particle types and conditions in the case that additional data can be obtained. Priorities should include: (1) environmental chamber and field studies with higher O:C values than available in the present study; (2) environmental chamber studies and field studies where the gradients of the isolines in Fig. 4 are steep and DRH and ERH are sensitive to specific O:C and org:sulf combinations; (3) direct measurements of liquid-liquid phase separation in environmental chamber studies and in the atmosphere; (4) laboratory studies of organic-ammonium sulfate particles that contain functional groups other than the ones used to develop the parameterisations presented here; and (5) studies using a broader range of composition, such as acidic particles or particles enriched in nitrate which are known to decrease ERH and DRH (Martin et al., 2003). Finally, the presented parameterisations were developed for oxygenated organics, non-oxygenated organic molecules (e.g., oily hydrocarbons), which on a global basis are less important than SOM, can still be important locally near or in urban centers (Kanakidou et al., 2005; Zhang et al., 2007; Hallquist et al., 2009). Studies of particles that have large concentrations of both oxygenated organic material and oily hydrocarbons are needed. The interesting story might develop further in such cases in that an additional phase separation might occur (i.e., three-phase liquid particles may form) (Knickerbocker et al., 1982). As a practical matter, the computational burden of the framework presented herein is low. Therefore, the parameterisations are well suited for incorporation in comprehensive chemical transport models (CTMs) (Wang et al., 2008). CTMs are used in large-scale predictions of atmospheric chemistry and are coupled in advanced treatments to global climate models. Future CTMs that incorporate predictions of O:C ratios alongside existing capabilities for organic and sulfate burdens may make use of these types of parameterisations for SRH, ERH, and DRH.

Supplementary material related to this article is available online at: http://www.atmos-chem-phys-discuss.net/11/17759/2011/ acpd-11-17759-2011-supplement.zip.

Acknowledgements. This research was supported by the National Sciences and Engineering Research Council of Canada (NSERC) and the USA National Science Foundation under Grant No. 0925467. Any opinions, findings, and conclusions or recommendations expressed in this material are those of the authors and do not necessarily reflect the views of the National Science Foundation. The authors thank K. A. R. Mitchell and K. C. Wong for assistance with the Raman Microscopy measurements.

References

Aiken, A. C., DeCarlo, P. F., and Jimenez, J. L.: Elemental analysis of organic species with electron ionization high-resolution mass spectrometry, Anal. Chem., 79, 8350–8358, 2007. 17788

Aiken, A. C., Decarlo, P. F., Kroll, J. H., Worsnop, D. R., Huffman, J. A., Docherty, K. S., Ulbrich, I. M., Mohr, C., Kimmel, J. R., Sueper, D., Sun, Y., Zhang, Q., Trimborn, A., Northway, M., Ziemann, P. J., Canagaratna, M. R., Onasch, T. B., Alfarra, M. R., Prevot, A. S. H., Dommen, J., Duplissy, J., Metzger, A., Baltensperger, U., and Jimenez, J. L.: O/C and OM/OC ratios of primary, secondary, and ambient organic aerosols with high-resolution time-of-flight aerosol mass spectrometry, Environ. Sci. Technol., 42, 4478–4485, 2008. 17762, 17769

Bodsworth, A., Zobrist, B., and Bertram, A. K.: Inhibition of efflorescence in mixed organic-inorganic particles at temperatures less than 250 K, Phys. Chem. Chem. Phys., 12, 12259–12266, 2010. 17763, 17781

Braban, C. F. and Abbatt, J. P. D.: A study of the phase transition behavior of internally mixed ammonium sulfate – malonic acid aerosols, Atmos. Chem. Phys., 4, 1451–1459, doi:10.5194/acp-4-1451-2004, 2004. 17762

Brooks, S. D., Wise, M. E., Cushing, M., and Tolbert, M. A.: Deliquescence behavior of organic/ammonium sulfate aerosol, Geophys. Res. Lett., 29, 1917, doi:10.1029/2002GL014733, 2002. 17762, 17780, 17781

Buzorius, G., Zelenyuk, A., Brechtel, F., and Imre, D.: Simultaneous determination of individual ambient particle size, hygroscopicity and composition, Geophys. Res. Lett., 29, 1974, doi:10.1029/2001GL014221, 2002. 17762

Chang, E. I. and Pankow, J. F.: Prediction of activity coefficients in liquid aerosol particles containing organic compounds, dissolved inorganic salts, and water - Part 2: Consideration of phase separation effects by an X-UNIFAC model, Atmos. Environ., 40, 6422–6436, 2006. 17767

Chen, Q., Farmer, D. K., Schneider, J., Zorn, S. R., Heald, C. L., Karl, T. G., Guenther, A., Allan, J. D., Robinson, N., Coe, H., Kimmel, J. R., Pauliquevis, T., Borrmann, S., Pöschl, U., Andreae, M. O., Artaxo, P., Jimenez, J. L., and Martin, S. T.: Mass spectral characterization of submicron biogenic organic particles in the Amazon Basin, Geophys. Res. Lett., 36, L20806, doi:10.1029/2009GL039880, 2009. 17768, 17769, 17786

Chen, Q., Liu, Y. J., Donahue, N. M., E., S. J., and Martin, S. T.: Particle-phase chemistry of secondary organic material: Modeled compared to measured O:C and H:C elemental ratios provide constraints, Environ. Sci. Technol., in press, 2011. 17769

Ciobanu, V. G., Marcolli, C., Krieger, U. K., Weers, U., and Peter, T.: Liquid-liquid phase separation in mixed organic/inorganic aerosol particles, J. Phys. Chem. A, 113, 10966–10978, 2009. 17762, 17763, 17765, 17767, 17780

Clegg, S. L., Seinfeld, J. H., and Brimblecombe, P.: Thermodynamic modelling of aqueous aerosols containing electrolytes and dissolved organic compounds, J. Aerosol Sci., 32, 713–738, 2001. 17762, 17767

Day, D. A., Takahama, S., Gilardoni, S., and Russell, L. M.: Organic composition of single and submicron particles in different regions of western North America and the eastern Pacific during INTEX-B 2006, Atmos. Chem. Phys., 9, 5433–5446, doi:10.5194/acp-9-5433-2009, 2009. 17763

DeCarlo, P. F., Kimmel, J. R., Trimborn, A., Northway, M. J., Jayne, J. T., Aiken, A. C., Gonin, M., Fuhrer, K., Horvath, T., Docherty, K. S., Worsnop, D. R., and Jimenez, J. L.: Field-deployable, high-resolution, time-of-flight aerosol mass spectrometer, Anal. Chem., 78, 8281–8289, 2006. 17769

Denbigh, K. C.: The Principles of Chemical Equilibrium, Cambridge University Press, Cambridge, 1981. 17767

Desnoyers, J. E. and Ichhaporia, F. M.: Salting-in and salting-out of polar nonelectrolytes, Can. J. Chem., 47, 4639–4643, 1969. 17766

Dibb, J. E., Talbot, R. W., Klemm, K. I., Gregory, G. L., Singh, H. B., Bradshaw, J. D., and Sandholm, S. T.: Asian influence over the western North Pacific during the fall season: Inferences from lead 210, soluble ionic species and ozone, J. Geophys. Res., 101, 1779–1792, 1996. 17762

Dibb, J. E., Talbot, R. W., and Scheuer, E. M.: Composition and distribution of aerosols over the North Atlantic during the Subsonic Assessment Ozone and Nitrogen Oxide Experiment (SONEX), J. Geophys. Res., 105, 3709–3717, 2000. 17762

Erdakos, G. B., Chang, E. I., Pankow, J. F., and Seinfeld, J. H.: Prediction of activity coefficients in liquid aerosol particles containing organic compounds, dissolved inorganic salts, and water - Part 3: Organic compounds, water, and ionic constituents by consideration of short-, mid-, and long-range effects using X-UNIFAC.3, Atmos. Environ., 40, 6437–6452, 2006. 17762

Finlayson-Pitts, B. J. and Pitts, J. N., J.: Tropospheric air pollution: Ozone, airborne toxics, polycyclic aromatic hydrocarbons, and particles, Science, 276, 1045–1052, 1997. 17761, 17763

Forster, P., Ramaswamy, V., Artaxo, P., Berntsen, T., Betts, R., Fa- hey, D. W., Haywood, J., Lean, J., Lowe, D. C., Myhre, G., Nganga, J., Prinn, R., Raga, G., Schulz, M., and Van Dorland, R.: Changes in Atmospheric Constituents and in Radiative Forcing, in: Climate Change 2007: The Physical Science Basis. Contribution of Working Group I to the Fourth Assessment Report of the IPCC, edited by: Solomon, S., Qin, D., Manning, M., Chen, Z., Marquis, M., Averyt, K. B., Tignor, M., and Miller, H. L., Cambridge University Press, Cambridge, United Kingdom and New York, NY, USA, 2007. 17762

Hallquist, M., Wenger, J. C., Baltensperger, U., Rudich, Y., Simpson, D., Claeys, M., Dommen, J., Donahue, N. M., George, C., Goldstein, A. H., Hamilton, J. F., Herrmann, H., Hoffmann, T., Iinuma, Y., Jang, M., Jenkin, M. E., Jimenez, J. L., Kiendler-Scharr, A., Maenhaut, W., McFiggans, G., Mentel, Th. F., Monod, A., Prévôt, A. S. H., Seinfeld, J. H., Surratt, J. D., Szmigielski, R., and Wildt, J.: The formation, properties and impact of secondary organic aerosol: current and emerging issues, Atmos. Chem. Phys., 9, 5155–5236, doi:10.5194/acp-9-5155-2009, 2009. 17762, 17763, 17769, 17771

Huebert, B. J., Howell, S. G., Zhuang, L., Heath, J. A., Litchy, M. R., Wylie, D. J., Kreidler-Moss, J. L., Coppicus, S., and Pfeiffer, J. E.: Filter and impactor measurements of anions and cations during the First Aerosol Characterization Experiment (ACE 1), J. Geophys. Res., 103, 16493–16509, 1998. 17762

Jayne, J. T., Leard, D. C., Zhang, X. F., Davidovits, P., Smith, K. A., Kolb, C. E., and Worsnop, D. R.: Development of an aerosol mass spectrometer for size and composition analysis of submicron particles, Aerosol Sci. Technol., 33, 49–70, 2000. 17762

Jimenez, J. L., Canagaratna, M. R., Donahue, N. M., Prevot, A. S. H., Zhang, Q., Kroll, J. H., DeCarlo, P. F., Allan, J. D., Coe, H., Ng, N. L., Aiken, A. C., Docherty, K. S., Ulbrich, I. M., Grieshop, A. P., Robinson, A. L., Duplissy, J., Smith, J. D., Wilson, K. R., Lanz, V. A., Hueglin, C., Sun, Y. L., Tian, J., Laaksonen, A., Raatikainen, T., Rautiainen, J., Vaattovaara, P., Ehn, M., Kulmala, M., Tomlinson, J. M., Collins, D. R., Cubison, M. J., Dunlea, E. J., Huffman, J. A., Onasch, T. B., Alfarra, M. R., Williams, P. I., Bower, K., Kondo, Y., Schneider, J., Drewnick, F., Borrmann, S., Weimer, S., Demerjian, K., Salcedo, D., Cottrell, L., Griffin, R., Takami, A., Miyoshi, T., Hatakeyama, S., Shimono, A., Sun, J. Y., Zhang, Y. M., Dzepina, K., Kimmel, J., Sueper, D., Jayne, J., Herndon, S. C., Trimborn, A. M., Williams, L. R., Wood, E. C., Middlebrook, A. M., Kolb, C. E., Baltensperger, U., and Worsnop, D. R.: Evolution of organic aerosols in the atmosphere, Science, 326, 1525–1529, 2009. 17762, 17768, 17769, 17786

Kanakidou, M., Seinfeld, J. H., Pandis, S. N., Barnes, I., Dentener, F. J., Facchini, M. C., Van Dingenen, R., Ervens, B., Nenes, A., Nielsen, C. J., Swietlicki, E., Putaud, J. P., Balkanski, Y., Fuzzi, S., Horth, J., Moortgat, G. K., Winterhalter, R., Myhre, C. E. L., Tsigaridis, K., Vignati, E., Stephanou, E. G., and Wilson, J.: Organic aerosol and global climate modelling: a review, Atmos. Chem. Phys., 5, 1053–1123, doi:10.5194/acp-5-1053-2005, 2005. 17763, 17771

King, S. M., Rosenoern, T., Shilling, J. E., Chen, Q., Wang, Z., Biskos, G., McKinney, K. A., Pöschl, U., and Martin, S. T.: Cloud droplet activation of mixed organic-sulfate particles produced by the photooxidation of isoprene, Atmos. Chem. Phys., 10, 3953–3964, doi:10.5194/acp-10-3953-2010, 2010. 17769

Knickerbocker, B. M., Pesheck, C. V., Davis, H. T., and Scriven, L. E.: Patterns of 3-liquid-phase behavior illustrated by alcohol-hydrocarbon-water-salt mixtures, J. Phys. Chem., 86, 393–400, 1982. 17771

Kwamena, N. O. A., Buajarern, J., and Reid, J. P.: Equilibrium morphology of mixed organic/inorganic/aqueous aerosol droplets: Investigating the effect of relative humidity and surfactants, J. Phys. Chem. A, 114, 5787–5795, 2010. 17765

Lee, L. L.: A molecular theory of Setchenov's salting-out principle and applications in mixedsolvent electrolyte solutions, Fluid Phase Equilibria, 131, 67–82, 1997. 17766

Lee, Y. N., Weber, R., Ma, Y., Orsini, D., Maxwell-Meier, K., Blake, D., Meinardi, S., Sachse, G., Harward, C., Chen, T. Y., Thornton, D., Tu, F. H., and Bandy, A.: Airborne measurement of inorganic ionic components of fine aerosol particles using the particle-into-liquid sampler coupled to ion chromatography technique during ACE-Asia and TRACE-P, J. Geophys. Res., 108, 8646, doi:10.1029/2002JD003265, 2003. 17762

Li, Y. J., Chen, Q., Guzman, M. I., Chan, C. K., and Martin, S. T.: Second-generation products contribute substantially to the particle-phase organic material produced by β-caryophyllene ozonolysis, Atmos. Chem. Phys., 11, 121–132, doi:10.5194/acp-11-121-2011, 2011. 17769

Liu, S., Takahama, S., Russell, L. M., Gilardoni, S., and Baumgardner, D.: Oxygenated organic functional groups and their sources in single and submicron organic particles in MILAGRO 2006 campaign, Atmos. Chem. Phys., 9, 6849–6863, doi:10.5194/acp-9-6849-2009, 2009. 17763

Marcolli, C. and Krieger, U. K.: Phase changes during hygroscopic cycles of mixed organic/inorganic model systems of tropospheric aerosols, J. Phys. Chem. A, 110, 1881–1893, 2006. 17762, 17780, 17781

Martin, S. T.: Phase transitions of aqueous atmospheric particles, Chem. Rev., 100, 3403–3453, 2000. 17762

Martin, S. T., Schlenker, J. C., Malinowski, A., Hung, H. M., and Rudich, Y.: Crystallization of atmospheric sulfate-nitrate-ammonium particles, Geophys. Res. Lett., 30, 2102, doi:10.1029/2003GL017930, 2003. 17770, 17771

Martin, S. T., Hung, H.-M., Park, R. J., Jacob, D. J., Spurr, R. J. D., Chance, K. V., and Chin, M.: Effects of the physical state of tropospheric ammonium-sulfate-nitrate particles on global aerosol direct radiative forcing, Atmos. Chem. Phys., 4, 183–214, doi:10.5194/acp-4-183-2004, 2004. 17761

Martin, S. T., Rosenoern, T., Chen, Q., and Collins, D. R.: Phase changes of ambient particles in the Southern Great Plains of Oklahoma, Geophys. Res. Lett., 35, L22801, doi:10.1029/2008GL035650, 2008. 17770, 17786

Murphy, D. M., Thomson, D. S., and Mahoney, T. M. J.: In situ measurements of organics, meteoritic material, mercury, and other elements in aerosols at 5 to 19 kilometers, Science, 282, 1664–1669, 1998. 17762

Murphy, D. M., Cziczo, D. J., Froyd, K. D., Hudson, P. K., Matthew, B. M., Middlebrook, A. M., Peltier, R. E., Sullivan, A., Thomson, D. S., and Weber, R. J.: Single-particle mass spectrometry of tropospheric aerosol particles, J. Geophys. Res., 11, D23S32, doi:10.1029/2006JD007340, 2006. 17762

Ng, N. L., Canagaratna, M. R., Zhang, Q., Jimenez, J. L., Tian, J., Ulbrich, I. M., Kroll, J. H., Docherty, K. S., Chhabra, P. S., Bahreini, R., Murphy, S. M., Seinfeld, J. H., Hildebrandt, L., Donahue, N. M., DeCarlo, P. F., Lanz, V. A., Prévôt, A. S. H., Dinar, E., Rudich, Y., and Worsnop, D. R.: Organic aerosol components observed in Northern Hemispheric datasets from Aerosol Mass Spectrometry, Atmos. Chem. Phys., 10, 4625–4641, doi:10.5194/acp-10-4625-2010, 2010. 17762, 17768, 17769, 17786

Pankow, J. F.: Gas/particle partitioning of neutral and ionizing compounds to single and multi-phase aerosol particles. 1. Unified modeling framework, Atmos. Environ., 37, 3323–3333, 2003. 17762

Pant, A., Fok, A., Parsons, M. T., Mak, J., and Bertram, A. K.: Deliquescence and crystallization of ammonium sulfate-glutaric acid and sodium chloride-glutaric acid particles, Geophys. Res. Lett., 31, L12111, doi:10.1029/2004GL020025, 2004. 17781

Pant, A., Parsons, M. T., and Bertram, A. K.: Crystallization of aqueous ammonium sulfate particles internally mixed with soot and kaolinite: Crystallization relative humidities and nucleation rates, J. Phys. Chem. A, 110, 8701–8709, 2006. 17763

Parsons, M. T., Knopf, D. A., and Bertram, A. K.: Deliquescence and crystallization of ammonium sulfate particles internally mixed with water-soluble organic compounds, J. Phys. Chem. A, 108, 11600–11608, 2004. 17762, 17780, 17781

Parsons, M. T., Riffell, J. L., and Bertram, A. K.: Crystallization of aqueous inorganic-malonic acid particles: Nucleation rates, dependence on size, and dependence on the ammonium-to-sulfate, J. Phys. Chem. A, 110, 8108–8115, 2006. 17762

Pope, C. A. and Dockery, D. W.: Health effects of fine particulate air pollution: Lines that connect, J. Air Waste Manage. Assoc., 56, 709–742, 2006. 17762

Pratt, K. A. and Prather, K. A.: Aircraft measurements of vertical profiles of aerosol mixing states, J. Geophys. Res., 115, D11305, doi:10.1029/2009JD013150, 2010. 17762

Ravishankara, A. R.: Heterogeneous and multiphase chemistry in the troposphere, Science, 276, 1058–1065, 1997. 17761

Rosenoern, T., Paulsen, D., and Martin, S. T.: The 1-by-3 tandem differential mobility analyzer for measurement of the irreversibility of the hygroscopic growth factor, Aerosol Sci. Technol., 43, 641–652, 2009. 17769

Russell, L. M., Bahadur, R., and Ziemann, P. J.: Identifying organic aerosol sources by comparing functional group composition in chamber and atmospheric particles, P. Natl. Acad. Sci. USA, 108, 3516–3521, 2011. 17763

Salcedo, D.: Equilibrium phase diagrams of aqueous mixtures of malonic acid and sulfate/ammonium salts, J. Phys. Chem. A, 110, 12158–12165, 2006. 17781

Seinfeld, J. H. and Pandis, S. N.: Atmospheric Chemistry and Physics, Wiley-Interscience, New Jersey, 2006. 17762, 17763

Sheridan, P. J., Delene, D. J., and Ogren, J. A.: Four years of continuous surface aerosol measurements from the Department of Energy's Atmospheric Radiation Measurement Program Southern Great Plains Cloud and Radiation Testbed site, J. Geophys. Res., 106, 20735–20747, 2001. 17770

Shilling, J. E., Chen, Q., King, S. M., Rosenoern, T., Kroll, J. H., Worsnop, D. R., McKinney, K. A., and Martin, S. T.: Particle mass yield in secondary organic aerosol formed by the dark ozonolysis of α-pinene, Atmos. Chem. Phys., 8, 2073–2088, doi:10.5194/acp-8-2073-2008, 2008. 17769

Shilling, J. E., Chen, Q., King, S. M., Rosenoern, T., Kroll, J. H., Worsnop, D. R., DeCarlo, P. F., Aiken, A. C., Sueper, D., Jimenez, J. L., and Martin, S. T.: Loading-dependent elemental composition of α-pinene SOA particles, Atmos. Chem. Phys., 9, 771–782, doi:10.5194/acp-9-771-2009, 2009. 17769

Smith, M. L., Kuwata, M., and Martin, S. T.: Secondary organic material produced by the dark ozonolysis of alpha-pinene minimally affects the deliquescence and efflorescence of ammonium sulfate, Aerosol. Sci. Technol., 45, 225–242, 2011. 17762, 17765, 17769

Talbot, R. W., Dibb, J. E., and Loomis, M. B.: Influence of vertical transport on free tropospheric aerosols over the central USA in springtime, Geophys. Res. Lett., 25, 1367–1370, 1998. 17762

Treuel, L., Schulze, S., Leisner, T., and Zellner, R.: Deliquescence behaviour of single levitated ternary salt/carboxylic acid/water microdroplets, Farad. Discuss., 137, 265–278, 2008. 17781

Treuel, L., Pederzani, S., and Zellner, R.: Deliquescence behaviour and crystallisation of ternary ammonium sulfate/dicarboxylic acid/water aerosols, Phys. Chem. Chem. Phys., 11, 7976–7984, 2009. 17781

Wang, J., Hoffmann, A. A., Park, R. J., Jacob, D. J., and Martin, S. T.: Global distribution of solid and aqueous sulfate aerosols: Effect of the hysteresis of particle phase transitions, J. Geophys. Res., 113, D11206, doi:10.1029/2007JD009367, 2008. 17771

Wise, M. E., Surratt, J. D., Curtis, D. B., Shilling, J. E., and Tolbert, M. A.: Hygroscopic growth of ammonium sulfate/dicarboxylic acids, J. Geophys. Res., 108, 4638, doi:10.1029/2003JD003775, 2003. 17762, 17780, 17781

Zhang, Q., Worsnop, D. R., Canagaratna, M. R., and Jimenez, J. L.: Hydrocarbon-like and oxygenated organic aerosols in Pittsburgh: insights into sources and processes of organic aerosols, Atmos. Chem. Phys., 5, 3289–3311, doi:10.5194/acp-5-3289-2005, 2005. 17768

Zhang, Q., Jimenez, J. L., Canagaratna, M. R., Allan, J. D., Coe, H., Ulbrich, I., Alfarra, M. R., Takami, A., Middlebrook, A. M., Sun, Y., Dzepina, K., Dunlea, E., Docherty, K., DeCarlo, P. F., Salcedo, D., Onasch, T., Jayne, J. T., Miyoshi, T., Shimono, A., Hatakeyama, S., Takegawa, N., Kondo, Y., Schneider, J., Drewnick, F., Borrmann, S., Weimer, S., Demerjian, K., Williams, P., Bower, K., Bahreini, R., Cottrell, L., Griffin, R. J., Rautiainen, J., Sun, J. Y., Zhang, Y. M., and Worsnop, D. R.: Ubiquity and dominance of oxygenated species in organic aerosols in anthropogenically-influenced Northern Hemisphere midlatitudes, Geophys. Res. Lett., 34, L13801, doi:10.1029/2007GL029979, 2007. 17762, 17763, 17768, 17771

Zuend, A., Marcolli, C., Peter, T., and Seinfeld, J. H.: Computation of liquid-liquid equilibria and phase stabilities: implications for RH-dependent gas/particle partitioning of organic-inorganic aerosols, Atmos. Chem. Phys., 10, 7795–7820, doi:10.5194/acp-10-7795-2010, 2010. 17762, 17766, 17767

Table 1. List of the data sets used for the parameterisations of SRH, ERH, and DRH in three-component systems (i.e. one organic plus ammonium sulfate and water). The DRH values reported here corresponds to the total DRH, which indicates where ammonium sulfate completely dissolves. For DRH and SRH we only included results from either bulk measurements or optical microscopy measurements because other techniques typically used for exploring the hygroscopic properties of aerosol particles can miss total deliquescence. For ERH we focused exclusively on optical microscopy measurements to be consistent with the new results reported in the current manuscript. Optical microscopy has been shown to be in good agreement in most cases with other techniques used to measure ERH properties of particles (Parsons et al., 2004). We also excluded any ERH results where it could not be shown that ammonium sulfate was the first solid to crystallise in the three-component particles. The complete data set is plotted in Fig. S1 as colour maps to illustrate that the data covers a wide range of org:sulf and O:C values without any large gaps in this phase space.

Compound	Formula	Functional Groups	O:C	Data Available
diethyl decanedioate	$C_{14}H_{26}O_4$	esters	0.29	ERH*, DRH*, SRH*
1,2-hexanediol	$C_6H_{14}O_2$	alcohols	0.33	DRH (Marcolli and Krieger, 2006), SRH (Marcolli and Krieger, 2006)
monomethyl octane-1,8-dioate	$C_9H_{16}O_4$	carboxylic acid-ester	0.44	ERH*, SRH*
1,4 butanediol	$C_4H_{10}O_2$	alcohols	0.50	DRH (Marcolli and Krieger, 2006), SRH (Marcolli and Krieger, 2006)
1,2,6-hexane-triol	$C_6H_{14}O_3$	alcohols	0.50	ERH*, DRH*, SRH*
4-dihydroxy-3-methoxybenzeneacetic acid	$C_9H_{10}O_5$	carboxylic acid-alcohols-ether-aromatic	0.56	ERH*, DRH*, SRH*
polyethylene glycol-400	$C_{2n}H_{4n+2}O_{n+1}$, $n = 8.2$ to 9.1	alcohols-ethers	~0.56	ERH (Ciobanu et al., 2009), DRH (Marcolli and Krieger, 2006), SRH (Marcolli and Krieger, 2006; Ciobanu et al., 2009)
2,5-dihydroxybenzoic acid	$C_7H_6O_4$	carboxylic acid-alcohols	0.57	ERH*, SRH*
hexanedioic acid	$C_6H_{10}O_4$	carboxylic acids	0.67	DRH (Brooks et al., 2002; Wise et al., 2003)
2,2-dimethylbutanedioic acid	$C_6H_{10}O_4$	carboxylic acids	0.67	ERH*, SRH*

Table 1. Continued.

Compound	Formula	Functional Groups	O:C	Data Available
pentanedioic acid	$C_5H_8O_4$	carboxylic acids	0.8	ERH (Pant et al., 2004), DRH (Brooks et al., 2002; Wise et al., 2003; Pant et al., 2004; Treuel et al., 2008, 2009), SRH*
6,8-dioxabicyclo[3.2.1]octane-2,3,4-triol	$C_6H_{10}O_5$	ethers-alcohols	0.83	ERH (Parsons et al., 2004), DRH (Parsons et al., 2004), SRH*
propane-1,2,3-triol	$C_3H_8O_3$	alcohols	1.00	ERH (Parsons et al., 2004), DRH (Parsons et al., 2004; Marcolli and Krieger, 2006), SRH*
L-hydroxybutanedioic acid	$C_4H_6O_5$	carboxylic acids	1.00	DRH (Brooks et al., 2002; Wise et al., 2003)
butanedioic acid	$C_4H_6O_4$	carboxylic acids	1.00	DRH (Brooks et al., 2002; Wise et al., 2003)
(*Z*)-butenedioic acid	$C_4H_4O_4$	carboxylic acids	1.00	DRH (Brooks et al., 2002; Wise et al., 2003; Treuel et al., 2009)
2-hydroxypropane-1,2,3-tricarboxylic acid	$C_6H_8O_7$	carboxylic acids-alcohol	1.17	ERH (Bodsworth et al., 2010), DRH (Bodsworth et al., 2010), SRH*
propanedioic acid	$C_3H_4O_4$	carboxylic acids	1.33	ERH (Parsons et al., 2004), DRH (Brooks et al., 2002; Wise et al., 2003; Parsons et al., 2004; Salcedo, 2006; Treuel et al., 2008, 2009), SRH*

[*] This study's data.

Table 2. Parameterisations of the SRH, ERH, and DRH data. In the parameterizations, terms include $x = \log_{10}$(org:sulf mass ratio) and $y =$ O:C atomic ratio.

Predictions	Parameterization	Valid Range	Reduced χ^2
SRH(x,y)	$= 0$	0.7 < (O:C) < 1.4 and 0.1 < (org:sulf) < 15	44.55
	$= 35.5 + 339.9y - 471y^2$	0.2 < (O:C) < 0.7 and 0.1 < (org:sulf) < 15	
ERH$(x,y)^*$	$= 144.6 + 207x - 217.1y + 138x^2 - 377.5xy + 84.87y^2 + 40.83x^3 - 220.8x^2y + 115xy^2 + 1.064x^4 - 58.79x^3y + 30.93x^2y^2 + 40.83x^3 - 220.8x^2y + 115xy^2 + 1.064x^4 - 58.79x^3y + 30.93x^2y^2$	0.7 < (O:C) < 1.4 and 0.1 <(org:sulf) < 15	2.62
	$= 33.99 - 1.098x - 0.166y$	0.2 < (O:C) < 0.7 and 0.1 < (org:sulf) < 15	
DRH(x,y)	$= 102.5 + 59.48x - 49.51y + 59.95x^2 - 110xy + 20.26y^2 + 28.83x^3 - 81.26x^2y + 32.68xy^2 + 3.077x^4 - 25.44x^3y + 10.44x^2y^2$	0.7 < (O:C) < 1.4 and 0.1 < (org:sulf) < 3	1.09
	$= 79.03 - 1.646x - 1.217y$	0.2 < (O:C) < 0.7 and 0.1 < (org:sulf) < 15	

* Negative ERH values correspond to the absence of efflorescence (i.e., no efflorescence is predicted even at 0 % RH).

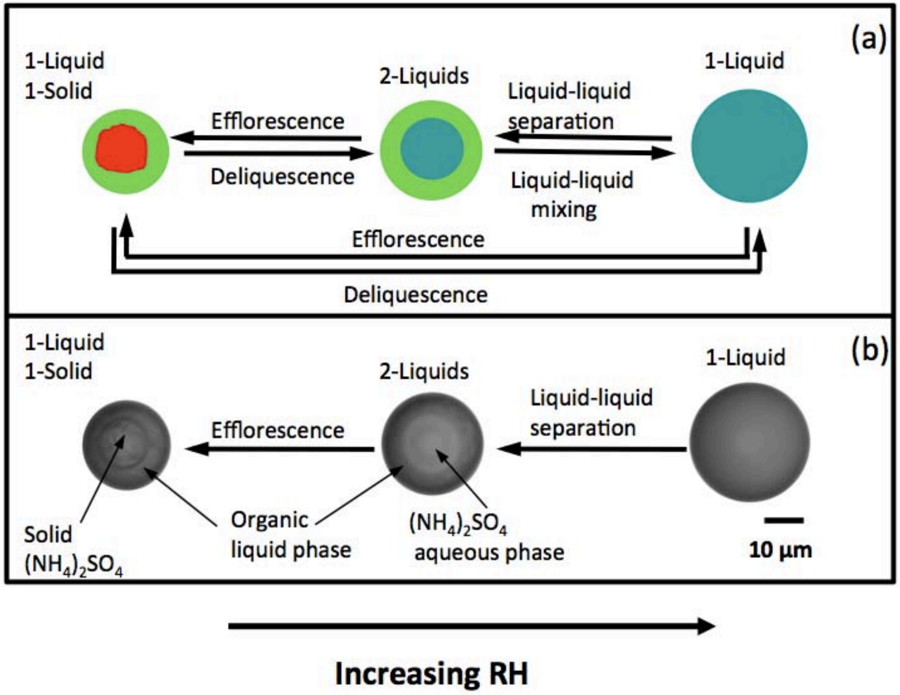

Fig. 1. **(a)** Some possible phase transitions of mixed organic-ammonium sulfate particles. These transitions can occur as atmospheric relative humidity fluctuates between high and low values. Aqua, green, and red respectively represent an aqueous phase, a liquid phase of organic material, and a solid phase of crystalline ammonium sulfate ($(NH_4)_2SO_4$). **(b)** Optical microscope images of a single particle consisting of 1,2,6-trihydroxyhexane and ammonium sulfate (org:sulf = 2.1) showing the sequence from right-to-left of an internally mixed liquid phase, two phase-separated liquids, and a core-shell arrangement of solid-liquid phase separation. Images were recorded using 500× magnification during a typical experiment as the relative humidity was decreased.

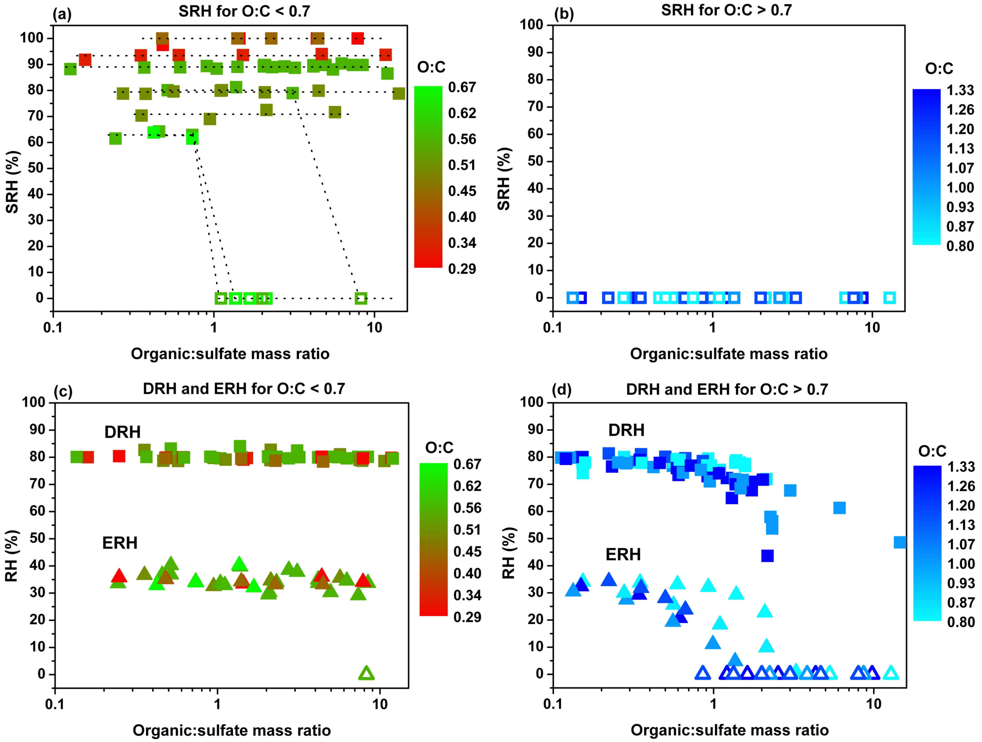

Fig. 2. Measurements of separation relative humidity (SRH), efflorescence relative humidity (ERH), and deliquescence relative humidity (DRH). Axes denote the observed relative humidity (RH) of a transition and the organic-to-sulfate mass ratio of a studied mixed system. Data are segregated between the left and right sets of panels for low (<0.7) and high (>0.7) oxygen-to-carbon (O:C) elemental ratios of the organic material. Open symbols indicate that no phase transition was observed. In some cases SRH was not probed below 35–40 % RH because ammonium sulfate or the organic material crystallised.

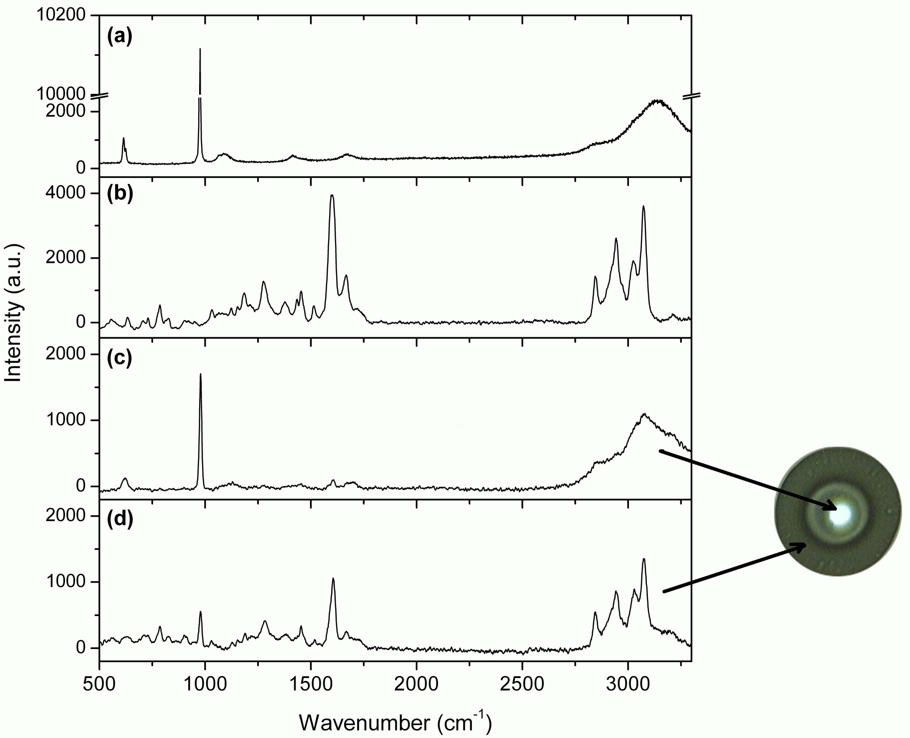

Fig. 3. Raman spectra of **(a)** a pure ammonium sulfate particle, **(b)** a pure 4-dihydroxy-3-methoxybenzeneacetic acid particle, **(c)** the core of a mixed 4-dihydroxy-3-methoxybenzeneacetic acid-ammonium sulfate particle after phase separation, and **(d)** the shell of a mixed 4-dihydroxy-3-methoxybenzeneacetic acid-ammonium sulfate particle after phase separation. The mixed particle used for Raman analysis is shown to the right.

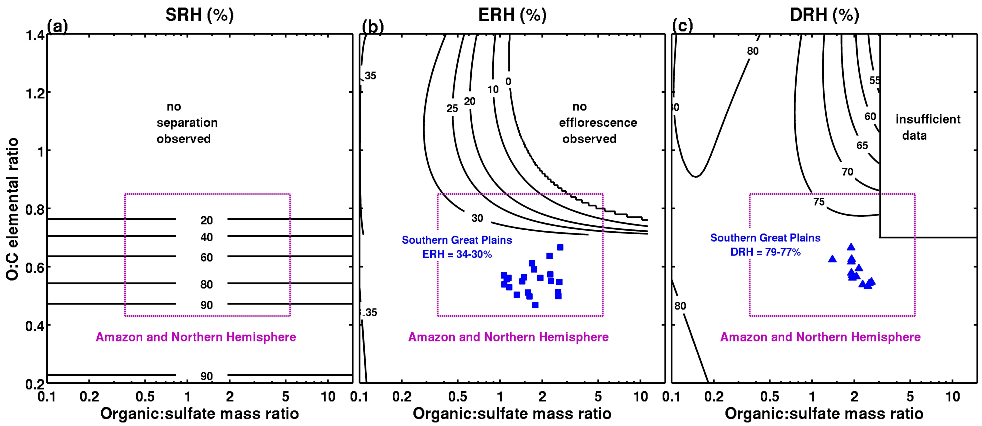

Fig. 4. Contour plots of SRH, ERH, and DRH based on the presented parameterisations of the experimental data. The magenta box encloses org:sulf and O:C values (campaign averages) measured in the pristine Amazon Basin (Chen et al., 2009) and many locations in the Northern Hemisphere (Jimenez et al., 2009; Ng et al., 2010). The blue symbols in **(b)** and **(c)** correspond to field measurements of ERH and DRH that were carried out at the Southern Great Plains (SGP), Oklahoma, USA (Martin et al., 2008). ERH and DRH measured at SGP are indicated in the figure. Since instruments commonly used to measure phase transitions in the field are not capable of directly measuring liquid-liquid phase separations, there are no field observations included in **(a)**.

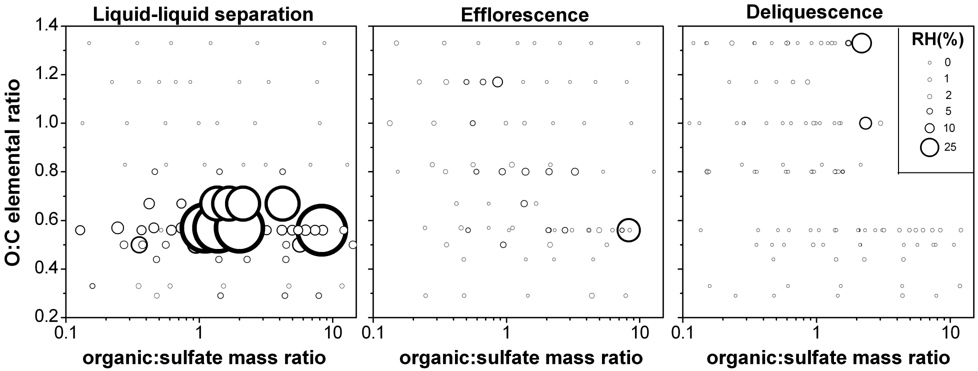

Fig. 5. The residuals (defined as the difference between parameterisations and measurements) for SRH, ERH, and DRH. The diameter of the circles correspond to the difference between the parameterisations and the measurements in % RH.

Title Page
Abstract | Introduction
Conclusions | References
Tables | Figures
|◀ | ▶|
◀ | ▶
Back | Close
Full Screen / Esc
Printer-friendly Version
Interactive Discussion

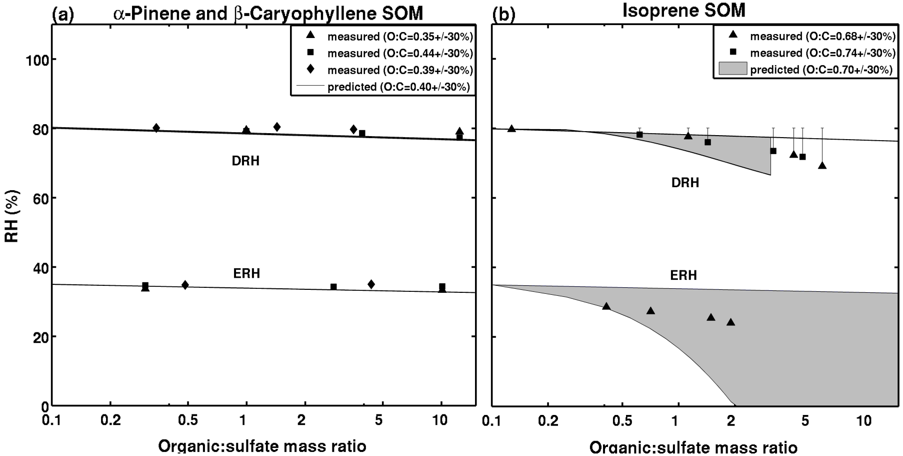

Fig. 6. Comparison between measured and predicted ERH and DRH for organic-sulfate particles. Panel **(a)** shows observations for organic material produced by the ozonolysis of *α*-pinene and *β*-caryophyllene. Panel **(b)** shows observations for organic material produced by isoprene photooxidation. The predictions shown in each panel represent the ERH and DRH parameterisations with input parameters of the measured org:sulf and O:C, including a maximum 30 % uncertainty in the O:C measurements (Aiken et al., 2007). This uncertainty is relatively less important for **(a)** (thus narrower bands) than **(b)** (wider bands) because of the different O:C values. The unsymmetrical error bars for the deliquescence measurements in **(b)** are discussed in the Supplement.